Targeted Correction of Point-Like Aberrations with High-Order Thermal Compensation

E. Bytyqi,[1] J. Richardson,[2] A. Brooks,[2] and R. Adhikari[2]
[1)]*Applied Physics and Applied Math Department, Columbia University, New York 10027 USA*
[2)]*LIGO Laboratory, California Institute of Technology, Pasadena, California 91125 USA*

(Dated: 27 September 2019)

Large scale interferometry has a crucial role in detecting gravitational waves which provide us with information about the early universe. The key to a good interferometer is its sensitivity which is proportional to the circulating power. LIGO uses Fabry-Perot cavities to ensure resonant power-build up and achieve high circulating power from a small input. However, due to point-like aberrations located at the end mirrors the amplitude of the resonant fundamental mode in the cavity is significantly limited. A large fraction of the circulating power is scattered into higher order modes which increase the cavity loss as they get closer to resonance. We propose a thermal compensation system consisting of a heater and a spherical reflector which reduces the effect of point absorbers by centrally heating the mirror at 1.9 cm wide spots.

I. INTRODUCTION

Large scale gravitational wave (GW) interferometers use Fabry-Perot cavities in a Michelson setup to detect GW events[1,2]. The importance of Fabry-Perot cavities is related to the resonant power build-up within the interferometer arms, increasing the sensitivity of the detector[3]. In an ideal case, the cavity consists of two perfectly spherical and highly reflective end mirrors which allow a very small portion of the light to be transmitted; the rest is reflected multiple times until resonance is reached. This results in an increased effective path length traveled by light and a higher circulating power in the arm. In the real case, however, the end mirrors are not perfectly spherical, significantly limiting the instrument's sensitivity. In order to maximize the gain from the resonant power build-up, the round-trip losses (RTL) from surface deformations on the cavity's end mirrors need to be minimized.

RTLs are caused by surface deformations that reflect light at large angles or by deformations which can couple the fundamental laser mode into higher order modes (HOMs). These HOMs behave in the same way as the fundamental mode, except at a different frequency. When a HOM reaches resonance inside the cavity, it increases the RTL, limiting the power that can be reached inside the interferometer arms. In the Advanced LIGO cavities, the 7th order mode generated by scattered light from the distortions on the test masses is the one closest to resonance and, therefore, the most problematic HOM. The cavities are designed to amplify an input power of 200 W to 750 kW[1]. However, due to point absorbers on the surface of the initial and end mirrors, the maximum arm power that can be obtained is 350 kW[4].

While the source of point absorbers remains unknown, they are nanometer-scale bumps on the LIGO test masses which absorb power from the laser at a higher rate than the rest of the surface. As they absorb more power the bump increases, amplifying the effect of the deformation. Although there have been several attempts at reducing RTLs caused by resonant HOM generation[5–8], none of the approaches directly tackles point absorbers.

In this study we examined a thermal compensation system (TCS) which locally heats up a mirror, decreasing the temperature gradient across its surface and reducing the effect of point absorbers. The tested TCS consisted of a cartridge heater and a spherical reflector of a certain radius of curvature which focused the radiant heat to a tight spot on an optic's surface. The design was built and optimized using finite-element analysis software and then assessed in the lab using a Hartmann Wavefront Sensor to quantify the surface deformation produced by the heating pattern. Our findings indicate that an array of these heating elements and reflectors can be used in targeted correction of point-like aberrations.

II. ROUND TRIP LOSSES DUE TO HOM RESONANCE

In order to study the effect of HOM resonance on the RTLs and to quantify the effect of the TCS, we need to compute the amplitude of each HOM inside the cavity[9]. In an ideal cavity where both end mirrors are perfectly spherical, the field inside it is expressed in terms of Hermite-Gauss modes as:

$$\Psi(x,y) = \sum_{m,n} \psi_{mn} HG_{mn}(x,y) \tag{1}$$

where $\Psi(x,y)$ is the complex field in terms of the transverse coordinates and ψ_{mn} is the field expansion coefficient in terms of the cavity eigenmodes[9]. In a real Fabry Perot cavity, the surface of the mirrors is distorted from the ideal spherical model by a function of the transverse coordinates z(x,y)[9]. The reflected field is expressed as:

$$\Psi_r(x,y) = 2ikr \sum_{mn} K_{mn} \psi_{00} HG_{mn}(x,y) \tag{2}$$

where $k = 2\pi/\lambda$, and r is the amplitude reflectivity of the end mirror, and K_{mn} is the coupling coefficient of the fundamental HG_{00} mode into the higher order HG_{mn} modes[9]:

$$K_{mn} = \int\int HG^*_{mn}(x,y) z(x,y) HG_{00} dx dy \tag{3}$$

As the light is being scattered into a HOM and reflected from the mirror, it gains an additional phase term called the Guoy

phase which depends on the length of the cavity (L) and the mirror's radius of curvature ($R_{1/2}$).

$$\Phi_g = (m+n)2arccos(\sqrt{(1-\frac{L}{R_1})(1-\frac{L}{R_2})} \quad (4)$$

Accounting for aberrations in only one of the mirrors, the amplitude of TEM_{mn} is:

$$a_{nm} = \alpha \frac{ir_1 r_2 e^{-2i\Phi+2i\Phi_{mn}}}{1-r_1 r_2 e^{-2i\Phi+2i\Phi_{mn}}} \frac{t_1}{1-r_1 r_2 e^{-2i\Phi}} a_{00} \quad (5)$$

where a_{00} is the amplitude of the incident field, $t_{1/2}$ is the amplitude transmissivity, $\alpha = 2kK_{mn}$, and $\Phi = -kL + \Phi_g$[10].

III. ADAPTIVE OPTICS APPROACH

The primary objective of this experiment was to focus a source of radiant heat to a point near the center of a test optic. While initially we considered using horns and elliptic reflectors to get a better focus, we decided to work on a design for a spherical reflector due to easier manufacturing.

A. Finite-element analysis

Before setting up the experiment, we used COMSOL to simulate our design and obtain preliminary results. The simulation consists of a cartridge heater placed just outside the mirror's front surface at a distance z above the optic. A spherical reflector is wrapped around it focusing the radiant heat roughly at the mirror's center (see Figure 1).

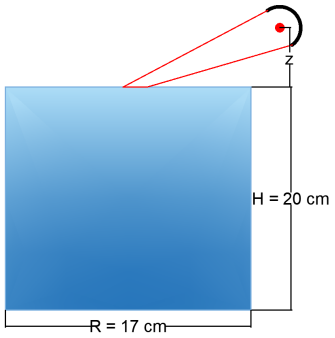

FIG. 1: (color online) Side view of the heater-reflector setup

The size of the test mass and the radius of the heater are fixed. The distance of the heater from the optic and the reflector's radius of curvature are parameters that need to be optimized. Additionally, the 2D geometry of the reflector resembles that of an arc which was varied from quarter to semi-circle. We found that a semi-circular arc focuses more energy which results in a higher surface temperature, whereas a quarter-circle arc obtains a tighter focus but loses a significant amount of energy. Due to the heater's radiation in all directions, the semi-circular cut is able to reflect more of the rays at a broader focus. At 25W source power from the ring heater, there is a 1 Kelvin difference between the peaks produced by semi-circular and quarter-circle reflectors.

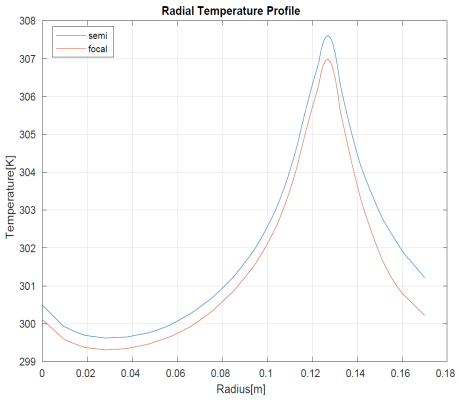

FIG. 2: (color online) Radial temperature profile for a semi-circle and quarter-circle reflector

The distance of the heater from the reflector was determined using ABCD matrices[11][12]:

$$\begin{bmatrix} 1 & L_2 \\ 0 & 1 \end{bmatrix} \begin{bmatrix} 1 & 0 \\ \frac{-2}{R} & 1 \end{bmatrix} \begin{bmatrix} 1 & L_1 \\ 0 & 1 \end{bmatrix} = \begin{bmatrix} \frac{R-2L_2}{R} & \frac{L_1(R-2L_2)+RL_1}{R} \\ \frac{-2}{R} & \frac{-2L_1+R}{R} \end{bmatrix} \quad (6)$$

where L_1 is the distance from the heater to the reflector and L_2 is the distance from the reflector to the test optic (at a point 5 cm away from the center). Setting $B = 0$ we can neglect the slope[13] and obtain an expression for $L_2 = \frac{-RL_1}{R-2L_1}$. To optimize the focus of the reflector we ran the model in MATLAB using different parameters. The best focus was achieved by ROC of 2.75 cm - 3.25 cm at a height of z = 3 cm rotated 30 degrees counter-clockwise. The COMSOL model assumes a gold-coated reflector and a heat source of 100W.

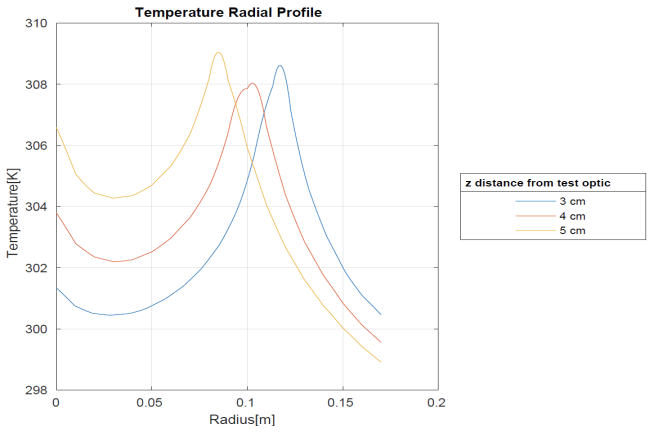

FIG. 3: (color online) Radial Temperature Profile produced by placing the reflector at different z values from the optic

B. Experimental Setup

In order to analyze the surface deformation of a test optic caused by focused heating, we set up a 2-lens system (see Figure 4) which collimates a laser beam to a radius of 2.5 cm, goes through the test optic (10 cm diameter) and is focused to a spot of r = 0.6 cm in order to fit the CCD aperture of the Hartmann Wavefront Sensor (HWS).

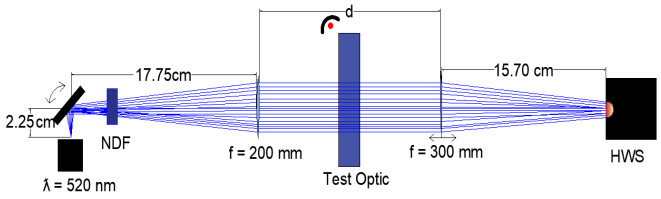

FIG. 4: (color online) Optical setup to test the effect of the TCS by analyzing the wavefront curvature with a HWS

A neutral density filter (NDF) was used to account for the saturated pixels of the sensor. The beam's angle of divergence, $\theta = 0.125$ rad was calculated by measuring the beam radius at 2 different points on the propagation axis. The focal length of the lenses and their position were chosen using paraxial ray approximation (see Eq. 6-9).

$$\begin{bmatrix} y_1 \\ \theta_1 \end{bmatrix} = \begin{bmatrix} 1 & 0 \\ -\frac{1}{f_1} & 1 \end{bmatrix} \begin{bmatrix} 1 & d_1 \\ 0 & 1 \end{bmatrix} \begin{bmatrix} y_0 \\ \theta_0 \end{bmatrix} \tag{7}$$

$$\begin{bmatrix} y_2 \\ \theta_2 \end{bmatrix} = \begin{bmatrix} 1 & d_2 \\ 0 & 1 \end{bmatrix} \begin{bmatrix} 1 & 0 \\ -\frac{1}{f_2} & 1 \end{bmatrix} \begin{bmatrix} y_1 \\ \theta_1 \end{bmatrix} \tag{8}$$

Here y_0, θ_0 are the parameters at the source, y_1, θ_1 are after the first lens, and y_2, θ_2 are at the CCD aperture. Solving for $y_0 = 0$ and $\theta_0 = 0.125$ rad, in order to collimate the beam ($\theta_1 = 0$), the distance of the first lens from the beam source must equal its focal length ($f_1 = d_1$).

$$\begin{bmatrix} y_1 \\ \theta_1 \end{bmatrix} = \begin{bmatrix} d_1\theta_0 \\ \frac{\theta_0(f_1 - d_1)}{f1} \end{bmatrix} \tag{9}$$

The beam's divergence angle and the desired radius of the collimated beam (y = 2.5 cm) determine the focal length of the first lens (f_1 = 200 mm). Similarly, we determine the focal length of the second lens (f_2 = 300 mm) to focus the beam to a radius of y_2 = 0.6 cm. To heat the test optic, we used a 31 mm long cartridge heater of 3 mm diameter. We powered it with a 120 V AC power supply, running 180 mA of current through it. The reflectors are semi-cylindrical with a height of 31 mm to fit the heater inside. We tested different ROCs for the reflector: 2.54 cm, 3.175 cm, and 3.81 cm. They were coated with Aluminum foil.

The Hartmann Wavefront Sensor was used to measure the optical path distance of the wavefront, providing information about the surface deformation of the test optic[7]. Using this data, we calculated the overlap integrals of higher order modes to determine how much power is being lost through scattering[14]. Additionally, we used a FLIR camera to characterize the heat distribution produced by the heater-reflector system and compare it to the simulated temperature profiles obtained on COMSOL.

IV. RESULTS AND DISCUSSION

The COMSOL model showed that a semi-circular reflector reaches higher temperatures than the quarter-circle reflectors, while the latter obtains a tighter focus. We tested this in the lab and measured the heat distribution produced by the different models at a distance of about 10 cm away from the target. The heat profiles showed that the quarter-circle reflector reaches a higher temperature and a tighter focus (full-width half-max = 1.9 cm), while the semi-circular one had a quite wide focus (FWHM = 3 cm).

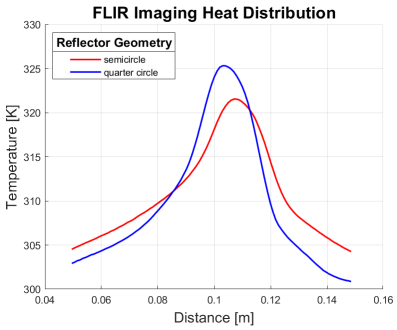

FIG. 5: (color online) Heat distribution profile of semi- and quarter- circle reflector

The distribution was imaged onto a piece of paper (see Figure 6) for qualitative analysis and comparison to the HWS wavefront profile.

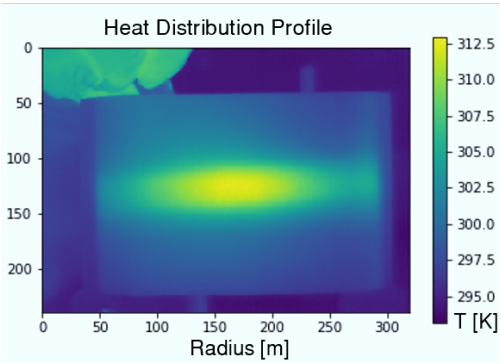

FIG. 6: (color online) FLIR image of heat profile produced by cartridge heater at 10 cm away from measurement point

Due to the design of the cartridge heater, most of the power was concentrated in the center which causes a "fade-out" at the ends. This can be fixed by using a reflector which is tighter and reflects back the heat radiated from a segment of

the heater. This could potentially form an even tighter focus in the horizontal direction.

The TCS was tested on the optical setup in Figure 4 where the HWS was used to take measurements of the wavefront profile both in the cold (laser turned on, heater off) and hot (laser and heater turned on) cases.

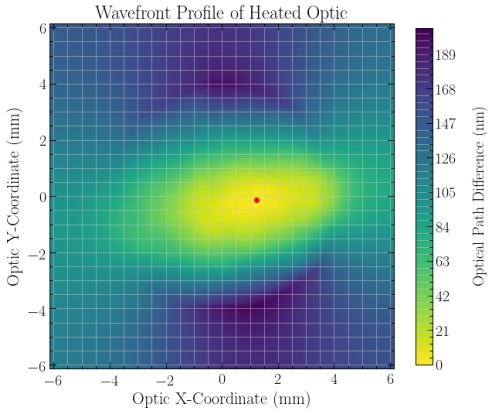

FIG. 7: (color online) Wavefront curvature profile of test optic heated with semi-circular reflector

The same "fade-out" pattern is observed in the HWS and that is due to the heater's structure. It still forms a focused heat pattern of 1.5 cm, which was the initial goal of the design.

V. CONCLUSIONS AND FUTURE WORK

A quarter-circle reflector obtains a tighter focus for a heating spot, however due to easier manufacturing of semi-circular reflectors we propose to use these in future tests and designs. The difference in focus tightness can be improved by a change of few parameters.

The design for a spherical reflector was successful in focusing heat to a 1.9 cm spot on an optic's surface. This pattern can further be reshaped and used for targeted actuation of HOM generation due to point absorbers on the ETM surface. Further testing and parameter optimization are necessary in obtaining an efficient TCS. Additionally, LIGO's noise requirements and vacuum compatibility need to be accounted for when building the real model. Eventually, an array of these heating elements could be used to produce heating patterns with several degrees of freedom allowing for actuation of several HOMs.

VI. ACKNOWLEDGEMENTS

I would like to thank my mentors Rana Adhikari, Aidan Brooks, and Jonathan Richardson for their help and guidance through all parts of the study, as well as LIGO Lab and Caltech for the equipment and resources.

[1]"LIGO's Interferometer," `https://www.ligo.caltech.edu/page/ligos-ifo`, accessed: 2019-06-25.
[2]T. P. Cheng, *Relativity, Gravitation and Cosmology* (Oxford University Press, 2010).
[3]R. X. Adhikari, "Gravitational radiation detection with laser interferometry," arXiv:1305.5188v3 (2014).
[4]A. Brooks, G. Vajente, D. Brown, H. Yamamoto, E. Hall, M. Kasprzack, and others, "The point absorbers," (2019), G1900203-v3 (unpublished).
[5]M. Smith and P. Willems, "Auxiliary optics support system conceptual design document, vol. 1 thermal compensation system," (2007), lIGO-T060083-01-D.
[6]P. Willems, "Heating of the itm by the compensation plate in advanced ligo," (2007), lIGO-T070123-02-D.
[7]J. T. Baker, F. Barone, E. Calloni, R. De Rosa, L. Di Fiore, L. Milano and S. Restaino, "An adaptive optics approach to the reduction of misalignments and beam jitters in gravitational waves interferometers," Classical Quantum Gravity Unpublished.
[8]A. Allocca, A. Gatto, M. Tacca, R. A. Day, M. Barsuglia, G. Pillant, C. Buy, and G. Vajente, "Higher-order Laguerre-Gauss interferometry for gravitational-wave detectors with in situ mirror defects compensation," Physical Review D (2015).
[9]G. Vajente, "In situ correction of mirror surface to reduce round-trip losses in fabry-perot cavities," Applied Optics **53** (2014).
[10]A. F. K. S. C. Bond, D. Brown, "Interferometer techniques for gravitational-wave detection," (2015).
[11]H. Kogelnik and T. Li, "Laser beams and resonators," Proceedings of the IEEE. **54** (1966).
[12]"Abcd matrix," `https://www.rp-photonics.com/abcd_matrix.html`.
[13]T. G. G. Eden, "Optical resonator modes," Presentation (unpublished).
[14]M. A. Arain, V. Quetschke, J. Gleason, L. F. Williams, M. Rakhmanov, J. Lee, R. J. Cruz, G. Mueller, D. B. Tanner, and D. H. Reitze, "Adaptive beam shaping by controlled thermal lensing in optical elements," Applied Optics **46** (2007).
[15]E. D. Hall, "The effect of a point absorber in an arm cavity," (2019), (unpublished).